2011 American Control Conference
on O'Farrell Street, San Francisco, CA, USA
June 29 - July 01, 2011

Design and Experimental Validation of a Model-Based Injection Pressure Controller in a Common Rail System for GDI Engine

Alessandro di Gaeta, Giovanni Fiengo, Angelo Palladino and Veniero Giglio

Abstract— **Progressive reductions in vehicle emission requirements have forced the automotive industry to invest in research and development of alternative control strategies. All control features and resources are permanently active in an electronic control unit, ensuring the best performance in terms of pollutant emissions and power density, as well as driveability and diagnostics. A way to attain these goals is the adoption of Gasoline Direct Injection (GDI) engine technology. In order to assist the engine management system design, through a better performance of GDI engine and the Common Rail (CR) system, in this work an injection pressure regulation to stabilize the fuel pressure in the CR fuel line is proposed and validated via experiments. The resulting control strategy is composed by a feedback integral action and a static model-based feed-forward action whose gains are scheduled as function of fundamental plant parameters. The tuning of the closed loop performance is then supported by an analysis of the phase margin and the sensitivity function. Preliminary experimental results confirm the effectiveness of the control algorithm in regulating the mean value rail pressure independently from engine working conditions, i.e. engine speed and time of injection, with limited design effort.**

I. INTRODUCTION

The CR injection system technology has been originally introduced for diesel engines in order to achieve both the reduction of pollutant emissions enforced by international regulations and the improvement of performance required by the customers. The key device of this system is the common rail, i.e. a steel manifold where the fuel is kept at high pressure. The electronically controlled high pressure fuel injection system holds an important role concerning both the emission control strategy and the improvement of internal combustion engine performance [1], [2]. High pressure injection allows to finely atomize the fuel spray and to promote fuel and air mixing, resulting in significant combustion improvements [3], [4]. Hence the control of the injection pressure plays a fundamental role to achieve a better and better engine performance by respecting the current stringent emission regulations.

Recently, this technology has been extended to gasoline engines [5], [6] and significant improvements have been reached adopting more sophisticated and precise control methodologies. As an example, in [7] a controller is designed applying the Quantitative Feedback Theory (QFT) to the closed-loop system. It results in a controller robust to model uncertainties and external disturbances, having moreover a quantitative measure of the robustness achieved. Simulations and experiments on a one-cylinder diesel-dual-fuel engine have shown interesting performance of the proposed controller, compared to the traditional PID. In [8] an hybrid model of the Magneti Marelli Powertrain common-rail fuel-injection system for four-cylinders multijet engine has been presented. The hybrid controller is then compared with a classical regulator designed via mean value based approach.

Even though an increasing number of technical papers proposing advanced feedback control loop are available, the control of high pressure in commercial products is still based on open loop strategy based on open loop strategy using tables function of pressure. Using the open loop control, injection pressure value is selected directly according to the engine operating conditions. Obviously this approach requires a non negligible time and material resources to identify the pressure mapping, and the resulting maps need to be updated in order to fulfill future emission reduction and fuel economy requirements. On the other hand, when reliable and simple enough models of the pressure rail are available, costs and resources can be reduced by using model-based control strategies.

In [9] authors proposed a control oriented model of the rail pressure in the case of a 2 liters GDI spark ignition engine. The model is capable to predict the mean value rail pressure as a good compromise between accuracy and model complexity, resulting particulary amenable for the design of efficient control algorithms. The modeling approach presented in [9] is in this work exploited to design a simple but effective injection pressure control strategy to regulate the mean rail pressure. The control architecture is mainly composed by a model-based feed-forward controller coupled with an integral closed loop action. Parameters of both controllers are scheduled as function of engine speed and battery voltage to compensate model mismatch. The resulting control strategy is then experimentally tested to show its effectiveness.

The paper is outlined as follows: in Sec. II the common rail system and its control oriented model are described for the sake of completeness, then an analysis on the disturbances affecting the injection pressure is drawn in Sec. III, finally, before conclusions, the design of the injection pressure controller and its experimental validation are reported in Secs. IV and VI, respectively.

This work was supported by the Italian Ministry for University and Research in the framework of the FIRB projects.

A. di Gaeta and V. Giglio are with Istituto Motori, National Research Council, 80125 Napoli, Italy. E-mail: {a.digaeta, v.giglio}@im.cnr.it.

G. Fiengo and A. Palladino are with the Dipartimento di Ingegneria, University of Sannio, 82100 Benevento, Italy. E-mail: {gifiengo, angelo.palladino}@unisannio.it.

978-1-4577-0079-8/11/$26.00 ©2011 AACC

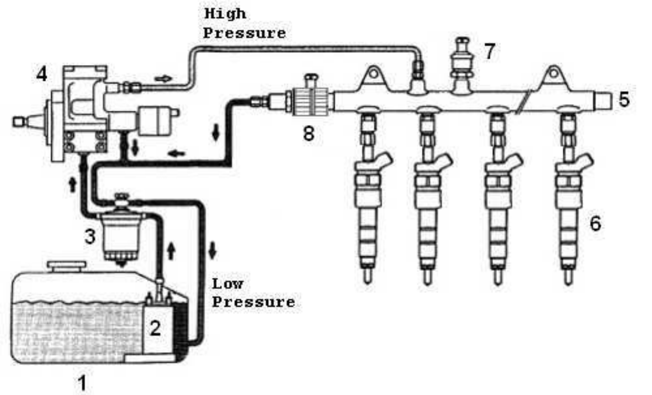

Fig. 1. Common rail injection system description: 1. fuel tank; 2. low pressure pump; 3. fuel filter; 4. high pressure pump; 5. common manifold; 6. electro-injector; 7. pressure sensor; 8. pressure regulation electro-valve.

II. Common Rail System

The main objective of a common rail system is to supply the electro-injectors with high pressure fuel independently by the amount to be injected. The main benefit is, therefore, to decouple the regulation of the pump by the functioning of the injectors, differently from traditional injection systems where the mechanical pump generates a pressure that depends on the amount of injected fuel.

The common rail plant for spark ignition engine, shown in Fig. 1, is composed mainly by two separated sections: a low-pressure circuit, consisting of a fuel tank, a fuel feed pump with a downstream filter, a low-pressure pipe and a fuel filter; an high-pressure circuit formed by a high-pressure pump, a high-pressure line with a pressure sensor, a pressure regulator valve, a flow stopper and the injectors. The low pressure electro-pump **(2)** $(4-5$ (bar)) forces the fuel from the tank **(1)** toward the high pressure mechanical pump **(4)** $(100-140$ (bar)), crossing the filter **(3)** aimed at cleaning the fuel. The second pump compresses the fuel and sends it into the common manifold **(5)** (named common-rail) equipped with the electro-injectors **(6)**. The manifold is designed in order to hold low the pressure oscillations in the fuel due to the pump and the intermittent working of the injectors. Finally, the pressure in the manifold is regulated through the sensor **(7)** and the electro-valve **(8)** that flows the excess of fuel back into the tank.

The high-pressure pump, shown in Fig. 2, is formed by three small pistons arranged in radial position (radial-jet) at an angular distance of $120°$. The pump is driven by the engine through the camshaft without the need of phasing since the start and duration of injection are imposed by the electronic control unit, which directly controls the opening of the injectors. The alternating movement of the three small pistons is assured by a triangular cam connected to the pump's shaft and each pumping group is characterized by an intake and exhaust valve. The combined action of the three pumping groups allows to reach a pressure in the range $20-100$ (bar), maintaining low level of residual pressure into the external manifolds.

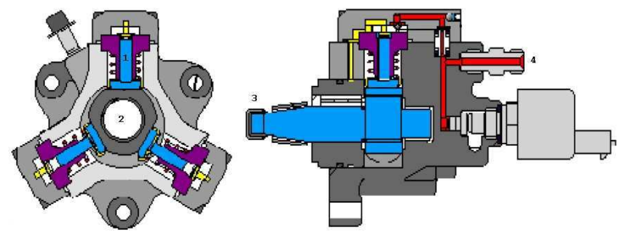

Fig. 2. High pressure pump scheme: 1) piston; 2) triangular cam; 3) shaft; 4) exit hole.

A. CR Mathematical Model

In order to control the injection pressure, a mathematical model is proposed in [9]. The model describes the electric dynamics of the electro-valve, neglecting the effects due to the plunger movement (i.e. inductance variations and back-electromotive force), and it considers the average pressure in the common rail as function of the high-pressure pump speed and electro-valve current. The model includes **the dynamics of** the actuation circuit used to drive the electro-valve, as well. In the following, the equations governing the behavior of the CR system are reported

$$\frac{di}{dt} = -\frac{R}{L} i + \frac{V_\mathrm{b}}{L}\left(\frac{a\delta(t)+b}{100}\right) \tag{1a}$$

$$\bar{p}(t) = c(N)i + d(N), \tag{1b}$$

where δ (%) (control input) is the duty-cycle expressed in percentage terms, i (A) (state) is the current, $\bar{p}$ (bar) (output) is the mean value of pressure in the common manifold, V_b (V) and N (rpm) (not manipulable inputs) are the battery voltage and the rotational speed of the high-pressure pump[1], respectively.

The parameters $c(\cdot)$ and $d(\cdot)$ in the output equation (1b) are modeled as function of the pump speed as follows

$$c(N) = \sum_{k=0}^{3} c_k \left(\frac{N}{10^3}\right)^k \quad \text{(bar/A)} \tag{2a}$$

$$d(N) = \sum_{k=0}^{3} d_k \left(\frac{N}{10^3}\right)^k \quad \text{(bar).} \tag{2b}$$

The values of the parameters are shown in Tabs. I e II. The model has been validated experimentally, comparing the simulated signals with measured data collected on a CR system of a 2.0 liters GDI engine. Further details on the model identification can be found in [9].

TABLE I
PARAMETERS OF THE STATE EQUATION

Parameter	Unit	Value
R	Ω	5.414
L	mH	18.74
a	-	1.0573
b	%	-5.6084

[1] $N = N_\mathrm{e}/2$ with N_e is the engine speed

TABLE II

PARAMETERS OF THE OUTPUT EQUATION

$c(N)$	Value	$d(N)$	Value
c_0	-97.9354	d_0	113.4366
c_1	-47.5405	d_1	41.8776
c_2	25.0493	d_2	-19.7275
c_3	-4.7962	d_3	3.5148

III. SYSTEM DISTURBANCE ANALYSIS

Here a study on the disturbances affecting the injection pressure is presented in order to help the design of the control strategy. This study starts from a theoretical analysis, validated subsequently by experimental data. In particular, in what follows two sources of disturbance will be considered.

Regarding the first, the voltage battery and the high-pressure pump speed, present in equations (1a) and (1b) respectively, are considered as measurable but not manipulable inputs. In particular, $V_{\mathrm{b}}(t)$ can be assumed slowly varying, except during the engine startup when the high energy requirements of the starter can cause a fast drop of the battery voltage. Conversely, $N(t)$ can suffer of high frequency variations being directly related to the engine speed, for instance during cranking phase, tip-in/out, cut-off and stop-and-go manoeuvres. Since these disturbances are both measurable, the adopted control law must be designed in order to adapt its action to reject, or at least to reduce, the negative effects of their variations.

Viceversa, more attention must be paid to design the control algorithm to balance disturbances causing pressure oscillations. To this aim, let consider the model (1b), describing the average manifold pressure when the injectors are not activated. In particular, the wave motion of the fuel into the rail, causing variations of the pressure, is completely neglected. It can be considered as a disturbance (in the following indicated as $\eta(t)$) to be added to the output of the model, returning so the instantaneous rail pressure

$$p(t) = \bar{p}(t) + \eta(t), \tag{3}$$

where $\eta(t)$ is composed mainly by two components: $\eta_{\mathrm{P}}(t)$, caused by the motion of the high-pressure pump, and $\eta_{\mathrm{I}}(t)$, caused by the functioning of the injectors.

The signal $\eta_{\mathrm{P}}(t)$ has zero mean since it is related to the pressure ripple caused by the pump. Conversely, $\eta_{\mathrm{I}}(t)$ has a continuous component that depends on the injection time T_{inj}, i.e. an increase of T_{inj} determines a reduction of the mass of fuel inside the manifold and, consequently, a reduction of the injection pressure.

Both components are periodic signals: $\eta_{\mathrm{P}}(t)$ is originated by the motion of the high-pressure pump, performing a round every two rounds of the engine crankshaft; $\eta_{\mathrm{I}}(t)$ related to the injectors functioning, activated sequentially one time for each engine cycle. Therefore, it is easy to find the frequencies of the fundamental harmonic components as follows:

$$f_{\mathrm{P}} = N/60 \tag{4a}$$

$$f_{\mathrm{I}} = nN/60, \tag{4b}$$

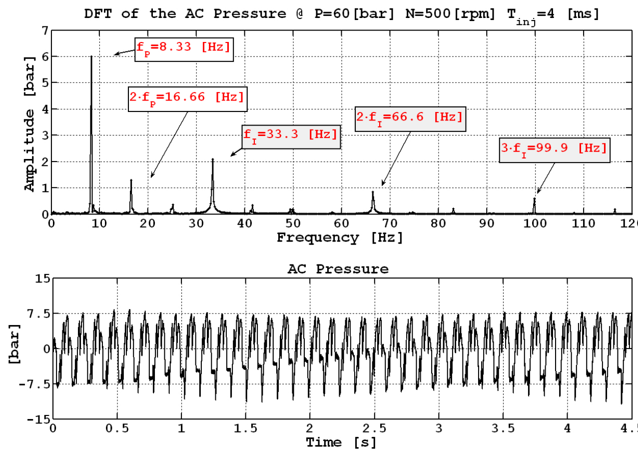

Fig. 3. Discrete Fourier Transformation (DFT) of common rail pressure @ $\bar{p} = 60$ (bar), $N = 500$ (rpm) and $T_{inj} = 4$ (ms).

where n is the number of injectors.

In order to validate this theoretical analysis, the spectrum of the measured injection pressure $p(t)$, collected for a 2.0 liters GDI engine at steady state condition ($\bar{p} = 60$ (bar), $N = 500$ (rpm) and 4 injectors activated for $T_{\mathrm{inj}} = 4$ (ms), is reported in Fig. 3. It is evident, in the first plot of the figure, that: **i)** the first harmonic components of $\eta_{\mathrm{P}}(t)$ and $\eta_{\mathrm{I}}(t)$, estimated at $f_{\mathrm{P}} = 8.33$ (Hz) and $f_{\mathrm{I}} = 33.3$ (Hz), agree with (4a) and (4b), respectively; **ii)** from the engineering viewpoint, it is possible to consider negligible the harmonic components for both disturbance terms over the 3rd to reconstruct satisfactorily the total pressure oscillations $\eta(t)$.

Based on these considerations, the disturbance $\eta(t)$ can be described as function of N and T_{inj} according to

$$\eta(t; N, T_{\mathrm{inj}}) = \eta_{\mathrm{P}}(t; N) - \eta_{\mathrm{I}}(t; N, T_{\mathrm{inj}}) \tag{5}$$

with

$$\eta_P(t; N) \approx \sum_{k=1}^{3} A_k^P \sin(\frac{\pi N}{30} kt + \varphi_k^P) \tag{6a}$$

$$\eta_I(t; N, T_{\mathrm{inj}}) \approx \alpha(T_{\mathrm{inj}}) + \sum_{k=1}^{3} A_k^I \sin(\frac{\pi N n}{30} kt + \varphi_k^I), \tag{6b}$$

where the amplitudes $A_k^{P,I}$ and the phases $\varphi_k^{P,I}$ of the sinusoidal terms are considered unknown parameters varying in general with N and T_{inj}, and where the following conditions can be reasonably and intuitively assumed: a) $\eta_{\mathrm{P}}(t; 0) = 0$ $\forall t$; b) $\eta_{\mathrm{I}}(t; N, 0) = 0$ $\forall N$; c) $\alpha(T_{\mathrm{inj}}) \geq 0$ with $\frac{d\alpha(T_{\mathrm{inj}})}{dT_{\mathrm{inj}}} > 0$ $\forall T_{\mathrm{inj}}$.

In [9] it has been experimentally observed that the disturbances (6) can be assumed bounded according to the following inequalities:

$$-0.543\bar{p}e^{-0.0229\bar{p}} < \eta_{\mathrm{P}}(t; N) < 0.853\bar{p}e^{-0.0296\bar{p}}, \tag{7}$$

for $N \leq 2500$ (rpm) and $\bar{p} \leq 100$ (bar);

$$\eta_{\mathrm{I}}(t; N, T_{\mathrm{inj}}) < 15, \tag{8}$$

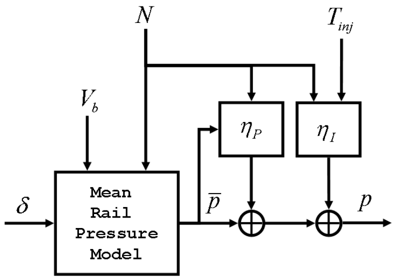

Fig. 4. CR plant to be controlled.

for $N \leq 2500$ (rpm), $\bar{p} \leq 100$ (bar) and $T_{\text{inj}} \leq 10$ (ms).

In Fig. 4 is reported the plant to be controlled, highlighting the disturbances acting on it.

IV. Pressure controller design

The controller objective is the mean value rail pressure to track a desired reference pressure, $p_{\text{d}}(t)$, according to the following set of control specifications: *i*) zero steady state error ($\bar{p}(\infty) = p_{\text{d}}$); *ii*) rise time lower then 250 (ms) ($t_s < 0.25$ (s)); *iii*) absence of elongations ($s_{\%} = 0$); *iv*) rejection of disturbance $\alpha(T_{\text{inj}})$, no amplification of harmonic components $A_k^{P,I}$ and fast compensation of the not manipulable inputs $V_b(t)$ and $N(t)$. Notice that, we suppose the reference to the control system is computed by a high level controller designed to optimize the engine performance in all operating conditions, but the design of a such a controller is out of the scope of the paper.

The proposed control strategy consists of two actions, i.e. a feed-forward action and a feedback action. The feed-forward controller is designed both to lead fast the injection pressure at the desired value and to limit pressure variations due to measurable disturbances

$$\delta_{ff}(p_d, \hat{V}_b, \hat{N}) = \frac{100R(p_d - d(\hat{N}))}{aV_b c(\hat{N})} - \frac{b}{a}, \tag{9}$$

where $\hat{V}_{\text{b}}$ and $\hat{N}$ are the measured battery voltage and pump speed, respectively.

The second action is provided by a closed loop controller with the aim of compensating unmodeled dynamics and reject unknown disturbances. In order to keep the control strategy as simple as possible, so that it is implementable in real-time applications with a low computational effort, we select as feedback controller an integral one with the following form:

$$C(s) = \frac{K_{\text{I}}}{s}, \tag{10}$$

with the gain K_{I} to be scheduled analytically on the basis of the not manipulable inputs.

To this aim, let consider the system transfer function, say $G(s)$, between the rail pressure and the feedback input computed in steady state condition (i.e. $\dot{V}_b = 0$ and $\dot{N} = 0$) when also the feed-forward action (9) feeds (1), which takes the following form

$$G(s) = \frac{K_g}{1 + s\tau}, \tag{11}$$

where

$$K_g(N, V_b) = \frac{aV_b c(N)}{100R} \tag{12a}$$

$$\tau = \frac{L}{R}. \tag{12b}$$

The closed loop transfer function when the feedback controller (10) is inserted in the loop is then[2]

$$W(s) = \frac{1}{s^2 \frac{\tau}{K_I K_g} + s\frac{1}{K_I K_g} + 1}. \tag{13}$$

At this point, we design the integral control gain, K_I , so that the closed loop dynamics (13) match those of a given linear system of the form

$$W_{\text{d}}(s) = \frac{1}{(1 + s\tau_{\text{d}})(1 + s\tau'_{\text{d}})}, \tag{14}$$

which is assumed to fulfill the control specifications. In particular, in order to meet control specification *iii*, the closed loop model (14) is selected as a second order linear time invariant system with zero step-response overshoot.

Now, the control problem has only one degree of freedom since it is easy to verify that: *j*) the model matching between (13) and (14) is feasible if and only if the following relation holds:

$$\tau'_{\text{d}} = \frac{\tau\tau_{\text{d}}}{\tau_{\text{d}} - \tau} \qquad \tau_{\text{d}} \in [2\tau; \infty[; \tag{15}$$

jj) the time constants are inverted for $\tau < \tau_d < 2\tau$; *jjj*) the solution does not exist for $\tau_d < \tau$.

Comparing (13) with (14), and taking into account (15), we derive the following expression for the integral gain:

$$K_{\text{I}}(\hat{V}_b, \hat{N}) = \frac{\tau_{\text{d}} - \tau}{K_{\text{g}}(\hat{N}, \hat{V}_b)\tau_{\text{d}}^2}. \tag{16}$$

Considering the control specification *ii*, for which it would be enough choosing $\tau_{\text{d}} \lesssim 114$ (ms), and taking into account that for condition *j* τ_{d} must be higher than $2\tau \approx 6.9$ (ms), a value of 100 (ms) (that in the worst case corresponds to 5 engine cycles at 6000 (rpm)) is finally set for τ_d. Hence, the second desired time constant τ'_{d} results 3.6 (ms).

Once obtained the controller, it is interesting to analyze the stability margins as function of τ_{d} and the sensitivity function. In particular, the phase margin increases with τ_{d}, as shown in Fig. 5a. For $\tau_{\text{d}} = 100$ (ms), it guarantees a phase margin $m_\varphi = 88$ (deg) for a crossover pulsation $\omega_{\text{t}} = 9.6$ (rad/s). The gain margin is ideally infinity.

The sensitivity function[3], again for $\tau_{\text{d}} = 100$ (ms), is shown in Fig. 5b. Notice that an attenuation of disturbance is guaranteed up to about 40 (rad/s).

The attenuation of $\eta_{\text{P,I}}$ disturbances can be extended to higher frequencies choosing carefully a lower value for τ_d, but the risk of inducing instability in the closed-loop system increases since the phase margin decreases with τ_d. For

[2] Sensor pressure dynamic has been neglected in $W(s)$ calculation. In fact, the sensor has time constant $\tau_s \approx 0.9$ (ms) with break pulsation $\omega_3 \approx 1100$ (rad/s).

[3] The sensitivity function is defined as $S(s) \triangleq \frac{E(s)}{N(s)} = \frac{1}{1+C(s)G(s)}$, where $N(s) = \mathcal{L}\{\eta(t)\}$.

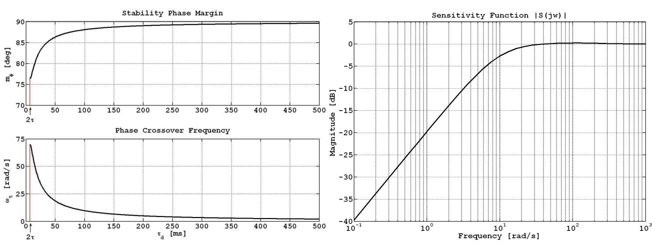

(a) (b)

Fig. 5. a) Phase margin in function of $\tau_{\rm d}$. b) Sensitivity function for $\tau_{\rm d} = 100$ (ms).

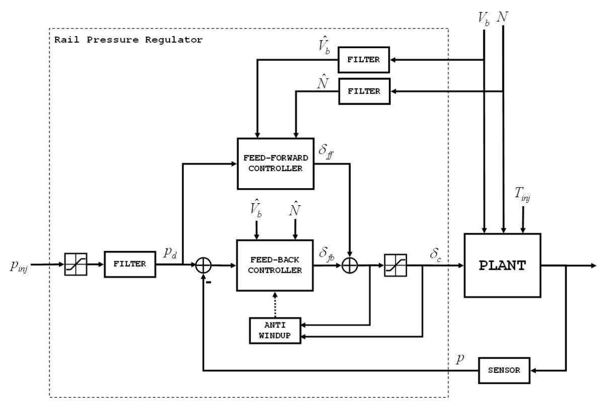

Fig. 6. Injection pressure controller scheme.

$\tau_d = 2\tau$ the cutoff frequency of sensitivity function could be moved up to 100 (rad/s), but at risk to have an amplification of $|S(jw)|$ in the range $100 - 1000$ (rad/s), where a peak of 1.25 (dB) at 200 (rad/s) would occur.

V. Experimental Setup

Experiments have been performed on a CR system of a 2 liters GDI spark ignition engine (see picture in [9]). The control strategy has been implemented according to the scheme in Fig. 6 and digitalized with a sampling time of $T_s = 5$ (ms).

The measurements of the voltage battery $V_{\rm b}(t)$ and pump speed $N(t)$ have been opportunely filtered to reduce the noise. Similarly, the desired pressure signal $p_{\rm d}$ has been preventively smoothed through a first order filter with a time constant equal to that desired ($\tau_{\rm d} = 100$ (ms)), so as to limit the tracking error during transients. The injection pressure, $p_{\rm inj}$, defined by an high level engine control strategy, has been limited into the interval $[p_{\rm low}; p_{\rm high}]$, where $p_{\rm low} = 5$ (bar) is the low pressure pump and $p_{\rm high} = 100$ (bar) is the maximum desired injection pressure. The integral action and all other filters have been digitalized via Tustin technique. Finally, the controller has been equipped with a back-calculation anti-windup mechanism since the control input δ can range in the interval $[0; 100]$.

VI. Experimental Results

Experiments have been carried out to highlight the performance achievable with the proposed control strategy. In particular, here we report the system response when both desired rail pressure and the injection time vary, while both the pump speed and battery voltage are instead kept constant at $N = 500$ (rpm) and $V_{\rm b} = 14.2$ (V), respectively. Moreover, as shown in Fig. 7, during the first 40 seconds the injectors are not active ($T_{\rm inj}(t) = 0$ and $\eta_{\rm I}(t) \equiv 0$), see Fig. 8, while during the last 85 seconds they become active ($T_{\rm inj}(t) > 0$ and $\eta_{\rm I}(t) \neq 0$), see Fig. 9.

In both cases, the controlled injection pressure signal satisfies the control specifications, i.e. rise time lower than 250 (ms), zero steady state error and the pressure peaks is limited into the interval of ± 10 (bar) of desired value. In Figs. 10 and 11 two details of the experiment during a pressure drop are shown, respectively when the injectors are inactive and then activated. Finally, in Fig. 12 the performance of the controller in steady state conditions during a wide and rapid variation of the injection time is shown. In this case we explicitly note that the proposed strategy controls the mean pressure at the reference but the injection time variations strongly alter the pressure ripples. Such unwanted effects could be reduced using advanced adaptive control methods, as confirmed by a numerical investigation [10].

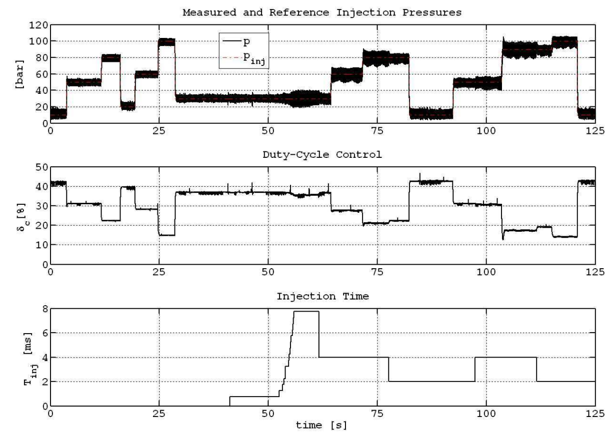

Fig. 7. Experimental test

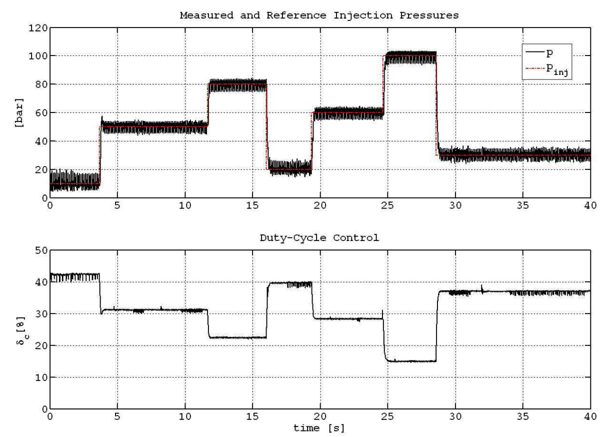

Fig. 8. Experimental test with injectors not active ($T_{\rm inj} = 0$ (ms)).

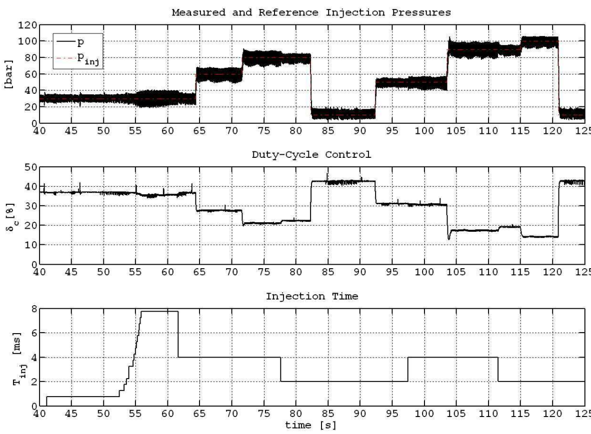

Fig. 9. Experimental test with active injectors ($T_{\text{inj}} > 0$ (ms)).

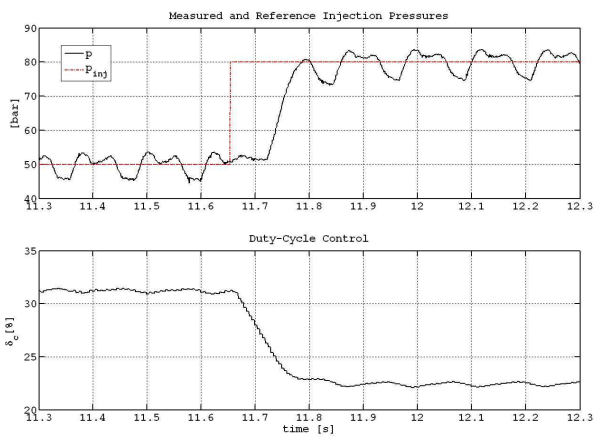

Fig. 10. Detail of the experiment: pressure drop in range $p = 50 - 80$ (bar) and $T_{\text{inj}} = 0$ (ms).

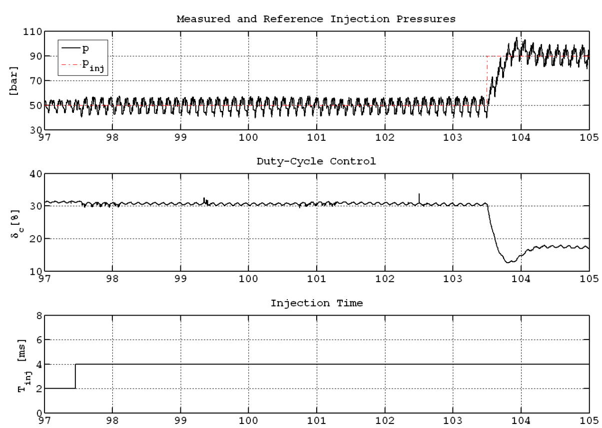

Fig. 11. Detail of the experiment: pressure drop in the range $50-90$ (bar) and injection time in the range $2 - 4$ (ms).

VII. CONCLUSIONS

In this work an injection pressure controller of a CR system for GDI engine has been presented. Based on a CR model previously presented in the literature by the authors, feed-forward and feedback control actions have been designed. The controller gains are scheduled in function of the HP pump speed and battery voltage, so providing an implicit adaptivity to all working conditions. The injection pressure controller has been successfully tested on a real CR injection system, proving to be able to keep the pressure oscillations within 10 (bar). A wide experimental analysis for testing the performance of the proposed model-based control strategy at higher engine speed (up to 6000 (rpm)) is now ongoing, and results will be presented elsewhere.

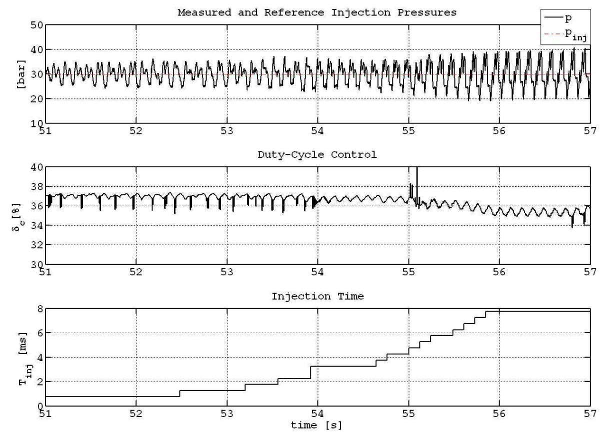

Fig. 12. Detail of the experiment: pressure regulated at 30 (bar) when injection time varies in the range $1 - 8$ (ms).

REFERENCES

[1] M. Fry, J. King, and C. White, "A comparison of gasoline direct injection systems and discussion of development techniques," *SAE Technical Paper*, no. 1999-01-0171, 1999.

[2] P. Lino, B. Maione, and A. Rizzo, "Nonlinear modelling and control of a common rail injection system for diesel engines," *Applied mathematical modelling*, vol. 31, no. 9, pp. 1770–1784, Sep. 2007.

[3] S. HaiFeng, Z. YouTong, W. Jun, and L. LianDa, "Researches of common-rail diesel engine emission control based on cylinder pressure feedback," in *Proc. of IEEE Vehicle Power and Propulsion Conference*, Haerbin, Heilongjiang, China, 2008.

[4] H. Tomishima, T. Matsumoto, M. Oki, and K. Nagata, "The advanced diesel common rail system for achieving a good balance between ecology and economy," *SAE Tecnical Paper*, no. 2008-28-0017, 2008.

[5] M. Corno, S. M. Savaresi, R. Scattolini, E. Comignaghi, M. Sofia, A. Palma, and E. Sepe, "Modelling, parameter identification and dynamics analysis of a common rail injection system for gasoline engines," in *Proc. of the 17th IFAC World Congress*, Seoul, South Korea, 2008.

[6] M. Tomforde, T. Jeinsch, J. Blath, and H. Dnow, "Modelling of a fuel supply system for model-based calibration," in *Proc. of the 17th IFAC World Congress*, Seoul, South Korea, 2008.

[7] W. Chatlatanagulchai, T. Aroonsrisopon, and K. Wannaton, "Robust common-rail pressure control for a diesel-dual-fuel engine using QFT-based controller," *SAE Technical Paper*, no. 2009-01-1799, 2009.

[8] A. Balluchi, A. Bicchi, E. Mazzi, A. L. S. Vincentelli, and G. Serra, "Hybrid modelling and control of the common rail injection system," in *Hybrid Systems: Computation and Control*, ser. Lecture Notes in Computer Science, J. Hespanha and A. Tiwari, Eds. Springer Berlin / Heidelberg, 2006, vol. 3927, pp. 79–92.

[9] A. di Gaeta, G. Fiengo, A. Palladino, and V. Giglio, "A control oriented model of a common-rail system for gasoline direct injection engine," in *Proc. of 48th IEEE Conference on Decision and Control & 28th Chinese Control Conference*, Shanghai, China, 2009.

[10] U. Montanaro, A. di Gaeta, and V. Giglio, "An MRAC approach for tracking and ripple attenuation of the common rail pressure for GDI engines," in *Proc. of the 18th IFAC World Congress*, Milan, Italy, Aug. 2011, accepted.